Journal of Engineering Science and Technology
Vol. 6, No. 2 (2011) 161 - 178

MIXING LOSSES INVESTIGATION DOWNSTREAM OF TURBINE BLADE CASCADE WITH COOLANT FLOW BLOWING

ASSIM HAMEED YOUSIF1,*, ABASS S. SHRIFFE[2]

[1]Mechanical Engineering Department, University of Technology,
P.O. Box 35010, Baghdad, Iraq
[2]Mechanical Engineering Department, University of Wassit, Kutt, Iraq
*Corresponding Author: assim_yousif2000@yahoo.com

Abstract

A major cause of noise and vibration characteristics of turbomachinery has caused by wakes. The characteristics of the wake, the wake decay, the path that it follows, and the mechanisms of mixing losses generated due to the mixing of blade trailing edge cold jet issued into the hot cross flow are important to find adequate solution to the problem. At the present work the wake characteristic was observed by introducing experimental work inside a cascade test rig to investigate the wake domain downstream of blade cascade with the aid of five-hole probe. The case studies were done with cold jets blowing ratios 1.58, 1.667 and 1.935 with jet stream wise angle and jet lateral injection angle 37.5° and 35° respectively. The measurement showed that there is a certain harmonization in the region of high reverse pressure loss coefficient which reflects the concentration of wake region. Also it was observed three distinct wake regions located in the centre of the passage vortex region. The wake characteristics measurements of the movement path, the growth of wake width, and the physical awareness of the wake propagating may help to explain the mechanisms of mixing losses.

Keywords: Mixing losses, Jet injection, Wake, Cascade, Blowing coolant, Five-hole probe.

1. Introduction

Blowing cooling works in the form of rows of jet holes in the spanwise directions of the blade, from where a cold jet is issued into the hot cross flow. Experimental investigations provide a clearer physical insight into the flow field downstream of the cascade. For two-dimensional flows, mixing usually only occurs in the wake or when boundary layers separate from the blade surface [1].

Nomenclatures

B	Bias (mean)
BR	Blowing ratio, U_{up}/V_j
C_p	Pressure coefficient
c	Blade chord, m
N	Number of samples
P	Pressure, Pa
P_1	Five-hole probe central tap pressure, Pa
P_2,P_3	Five-hole probe lateral tap pressure, Pa
P_4,P_5	Five-hole probe vertical tap pressure, Pa
P_r	Precision
s	Blade pitch, m
U	Mean velocity component in axial direction, m/s
U_n	Uncertainty
u, v, w	Component of velocity vectors in x, y, and z directions respectively, m/s
x	Axial downstream, m
x_{avg}	Mean of measured value
x_i	Downstream measured value of five-hole probe

Greek Symbols

β	Inlet flow angle, degree
δ	Standard deviation
σ	Cascade solidity

Subscripts

pitch	Five- hole probe pitch
t	Total pressure
s	Static pressure
up	Upstream
yaw	Five- hole probe yaw

Although it is only a relatively short-lived phenomenon as the flow eventually mixes out completely, it is a major contributor to the total loss, since it is normally associated with turbulent flows where the effect of viscosity is very large.

In particular, at high velocity the intense viscous dissipation immediately behind the trailing edge generates considerable. For a two-dimensional incompressible flow, the loss is reduced in an accelerating flow and increased in a decelerating flow; this effect is difficult to quantify, however, as mixing is a continuous process. The majority of the mixing loss occurs within 10 trailing edge thicknesses downstream [2], but the loss continues to rise for approximately one chord downstream of the blade row. The mixing loss will also be affected if the flow interacts with the downstream blade row before it has completely mixed out. Recent studies given by [3-5] analyzed the performance of such blowing cooling systems.

Turbine wakes represent a source of loss in efficiency, since the mixing of the wakes with the free stream dissipates energy. An understanding of the wake development and its decay is also essential because of the role it plays in the rotor-stator interaction.

2. Experimental Investigation

Experimental investigation designed to provide the possible understanding about the aerodynamic effect of the trailing edge blowing coolant flow on loss mechanisms. The description of the design procedure starts from the point where the blade section of the Low Pressure Turbine [LPT] is to be modelled. The same shape of thickness distribution of Langston blade geometry [6] in which linear cascade type is used. The cascade defined by the following parameters, the shape of the blade, cascade stagger angle, cascade solidity (σ) and inlet flow angle (β_1). To model the blade at low speed, more compromises are required such as low speed cascades, by virtue of their larger scale and lower speeds, offer several advantages over high speed cascades. In low speed cascades, the maximum size of the blades is determined by the need to keep the lowest Reynolds number the same as in the real machine and by the need to have measurable pressure differences when running at or close to atmospheric pressure at the low velocity the large scale implies. Table 1 shows the dimensions and the angles of the vane turbine blade which is used in present study to produce the cascade of LPT blade. Figure 1 shows the blade row attached to one side of end wall. The effects of heat transfer from the flow will not be considered in this study.

Table 1. The Dimensions and Angles for Blade.

Number of blades	5
Chord, mm	67
Axial chord, mm	62
Blade stagger angle, degree	24
Pitch, mm	60.47
Span, mm	61.2
Inlet flow angle, degree	44.7
Blade inlet angle, degree	43.99
Solidity	1.122
Aspect ratio	0.987
Blowing ratio	1.58,1.667, 1.935

Fig. 1. Blade Row attached to One Side of End Wall.

2.1. Wall jets

All wall jets have the same type and configuration. The holes were drilled ahead to the blade trailing edge at the pressure side, to hold fitting for 1 mm diameter jets. External injection is created by the air bled from the compressor stage, ducted through the internal chambers of the turbine blades, and then discharged through small holes (25 holes kinds' forward –lateral expanded hole). Each pitch distances between two neighboring holes are equals to three times of hole diameter. Figure 2 shows row of forward–lateral expanded holes located at the pressure side of the blade.

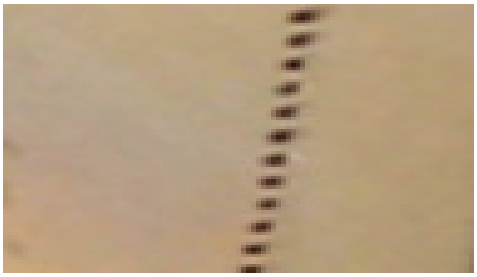

Fig. 2. Row of Forward–Lateral Expanded Holes located at the Pressure Side of the Blade Close to the Trailing Edge.

Jets velocity was controlled by a pressure regulator valve and flow meters are fixed near the air supply to insure that all jets have the same velocity**.** In typical gas turbine the optimized blowing ratios is within 0.8 to 2.0 [7]. The blowing ratios in present study are (1.58, 1.667and 1.935), the forward exit jet angle is 37.5^{o} as advised by [8] and the jet lateral angle was taken to as 35^{o}. Only at blowing ratio greater than 1 the jet was able to push main stream back and jet formed a solid protective layer in the shape of a rod. The common standard calibrations possible have been made to confirm the flow parameters in the test rig section.

2.2. Boundary correction

The conditions under which a model is tested in a test rig are not the same as those in free air. The effect of the walls and the model thickness and the wake are subjected to solid and wake blocking. Solid and wake blocking are usually negligible with an open test section, since the air stream is then free to expand in a normal manner [9]. The total solid and wake-blocking correction is calculated as the ratio of model frontal area to test section frontal area. As suggests by Maskel [10] the maximum ratio of model frontal area to test cross-sectional area of 7.5% should probably been used, unless errors of several percent can be accepted. In the present investigation, the cascade frontal area to the test cross-section area is equal to 4.1%. Thus, the blocking errors are very small and can be neglected.

2.3. Five-hole probe

A variety of pressure probes have been devised for decomposing the flow velocity vector. The devise is a stream lined ax-symmetric body that points into the flow. The pressure distribution on the surface of the probe depends on the incidence angle of the main flow vector relative to the axis of the probe. To determine the

magnitude and the orientation of the flow vector, the surface pressure is sampled at five locations; on the axis of the probe and at four equipage points on a line encircling this central point [11]. The pressure differentials between selected pairs of these points may be related to the inflow velocity vector by using an appropriate calibration to deduce pitch and yaw directions. Hypothetically, theoretical relationships for the potential flow around the body may also be used as given by Schuiz [12]. The conical tip head has been used in the present experimental program. Central pressure tap gives the conventional stagnation pressure when the flow vector is perpendicular to the point on the surface. Yaw and pitch angles inclinations of the flow vector with axis of the probe result in arm balance of pressure on pairs of hole. The theory yields a format for interpreting the differential pressures between pairs of holes is a function of the angles of pitch and yaw.

The accuracy of measurements is achieved by using the five-hole probe; the probe should be able to read velocities with 10% accuracy and angles within 5^{o} accuracy to be useful for data collection in a blade cascade. The measurement procedure of the uncertainly was done according to the procedure given by Kline and McClintock [13]. This approach estimates experimental value uncertainly by summing the squares of the contribution of error from measured quantities and taking the square root of the summation to provide the final uncertainly of the experimental values. The uncertainly calculations for the five-hole probe are identical to those of Drost [14]. Thus, the uncertainty was expressed in the following manner;

Standard deviation

$$\delta = \sqrt{\frac{1}{N}\sum_{i=1}^{N}\left(x_i - x_{avg}\right)^2} \tag{1}$$

where the precision (P_r) is given by ($P_r = 2\delta$), and the uncertainty (U_n) is given by $U_n = B + P_r$.

2.4. Five-hole probe calibration

The results of calibration were brought up here in order to illustrate the maps of the coefficients of pitch and yaw angles. It is essential to refer that one of the basic things in calibration of five-hole probe is the attempt to equalize between pressures lying on one plane which means (P_2 and P_3) in the horizontal plane and (P_4 and P_5) in the perpendicular plane. Figure 3 shows the five-hole probe and port numbering. Thus, trigger point for calibration and considered as a zero point for altering yaw and pitch angles. Therefore, the zero point for tips of five-hole probe has now been fixed on zero yaw and pitch angles. This will lead to manifest maps of total pressure coefficient and dynamic pressure coefficient.

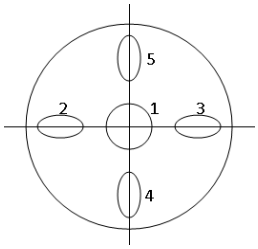

Fig. 3. Five-Hole Probe Ports Numbering.

These maps will be used to calculate the flow velocities downstream of blade cascade since the orientation of the probe, yaw and pitch angles have been calculated. In this experimental investigation the procedure of Charley [15] was used with small changes in the calculation of the average pressure sum of the four pressures reading P_2 to P_5, instead of taking the sum of smallest two pressures, since all the pressure taping varied during the calibration process, as indicated in the following equation;

$$P_{avg} = (P_2+P_3+P_4+P_5)\ /4 \tag{2}$$

The dimensionless pressure coefficients were used to process the five-hole probe data. These pressure coefficients were used to set out the required calibration curve of the five-hole probe, and they are plotted against the pitch and yaw angles as variable. Total pressure P_1 is measured at central probe hole, while P_2 and P_3 were measured in the yaw plane and P_4 and P_5 are measured in the pitch plane.

2.5. Two-dimensional measurement

A two-dimensional measurement grid was devoted for the region downstream of blade cascade starting from throat plane represented by the pitch distance. The mesh of planes parallel to the pitch plane were divided into ten mesh points with distance of 0.5 cm while the planes perpendicular to the axial one were divided into eleven points with distance of 1 cm. Finally the grid points will have a mesh of (10×11). Figure 4 shows the measurement location of the velocity components.

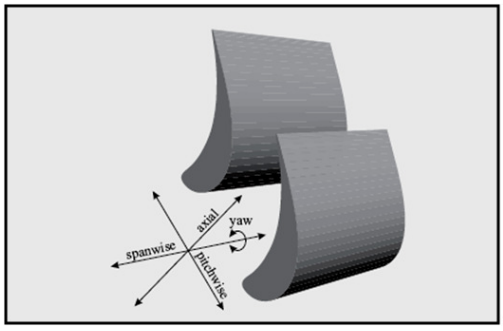

Fig. 4. Spanwise and Pitchwise Velocity Components Directions.

Experimental results are shown in two main articles, first one deals with calibration of five-hole probe data which outcomes by resolving of pressures reading obtained at a the free stream region upstream of blade cascade in which these data will be used again in the second article. Figure 5 illustrates the maps of pitch and yaw angles coefficients. The second articles will use the former mentioned data that scanned the downstream cascade region, which lies downstream of trailing edge. This process comprises partition of the downstream region into eleven planes parallel to each other and perpendicular to exit flow direction that leaving the throat area and passing through uncovered suction surface. As a consequence of this process, wake flow mixing region can now be

easily simulated through detailed survey of the partitions mentioned to reveal effects of losses, which rose from propagation of these wakes.

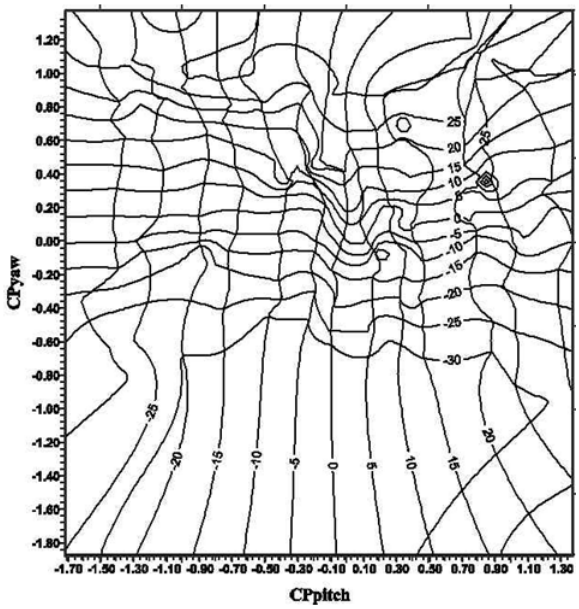

Fig. 5. Map of Pitch and Yaw Coefficients Angles.

The measurements of the cascade wake flow field were obtained for the matter of determining the characteristics of the blade cascade wake, including its movement path, the growth of its wake width, and the physical awareness of present problem. The blowing ratios in the present study were changed in order to understand the role of this change on the wake propagation and behaviour. The primary flow direction is defined in the direction of the mean camber line at the trailing edges of the blades ($\beta_2 = 26^o$). The velocity component in this direction is termed (u) and the secondary flow velocity components (v) and (w) have been thus defined in the cross-sectional plane. All the measurements performed on midspan orientation. A brief summary of the pressure parameters describes the wake behaviour is written below based on aerodynamic and losses equations:

$$C_{Ps} = \frac{P_{s_i} - P_{s_{up}}}{\frac{1}{2}\rho U_{up}^2} \tag{3}$$

$$C_{Pt} = \frac{P_{t_{up}} - P_{t_i}}{\frac{1}{2}\rho U_{up}^2} \tag{4}$$

3. Pressure Loss Coefficient Contours

Figures 6 to 8 show the variation of the minimum static pressure coefficient quantities which are -0.1, -0.35 and -1.3 respectively which are close to the pressure side and are -1,-2 and -2.5 at the suction side. From other point of view, the minimum loss region near the pressure side appears to be a two-dimensional

potential flow region. However, the other half of the flow is quite different as evidenced by nearly concentric static pressure contours surrounding the core of the passage vortex. The minimum value of C_{ps} in vortex core for three upstream velocities without blowing as it is obtained by [16] equals to, -1, -2 and -2.5 respectively. These results indicated that the static pressure coefficient reduced by (60%) if compared with static pressure coefficient resulting from blowing ratio (1.935) and by (50%) if compared with blowing ratio 1.58. In addition, the static pressure coefficient contours increase and have a large vortex core close to the suction surface when the blowing ratio is decrease. This maybe due to that the injection of the jets could not divert the forward movement of the mainstream, therefore the jets could not successfully push the path of the passage vortex and decrease its effect on the suction side of the blade. Since C_{ps} increases, so that the mixing losses increase, i.e., more generation of vortex core. The decrement in the blowing ratio possess additional wake flow as the flow progresses forward in the downstream direction, in the area lying above the midpitch, because the amount of turbulent intensity throughout blade passage and downstream of blade trailing edge increases. Accordingly, this may be associated with relation to the additional fluctuation of wake flow when the flow is accelerated and the kinetic energy increases with existing of shear layer between the regions.

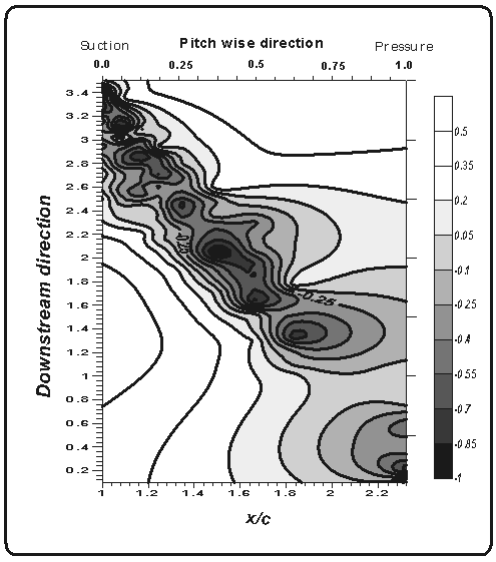

Fig. 6. Static Pressure Loss Coefficient Contours in Pitchwise Direction, BR (1.58).

Other point of view, obtained from these figures is that the expanding of wake flow regimes to overlap the area above midpitch line maybe attributed to the effect of passage of vortex and showed that the wake expanded by (0.65%), (0.45%) and (0.30%) in pitchwise direction. The inviscid core region, trailing filament and trailing shed vortices were worked as a continuous local source of momentum convection and surmount the regions with a positive velocity leading to large amount of momentum transfer between layers of both regions. The wake life distance in downstream are equal to 1.18c, 0.74c and 0.44c (where c is the blade chord) for the blowing ratio 1.58, 1.667 and 1.935 respectively.

The mixing losses of the flow field behind the blade trailing edge are normally associated with turbulent flows where the effective viscosity is very large. In particular, at high blowing ratio the intense viscous dissipation does not occurred immediately behind the trailing edge. Thus, due to these reasons explained why the wake live distance increasing with the increase of the blowing ratio.

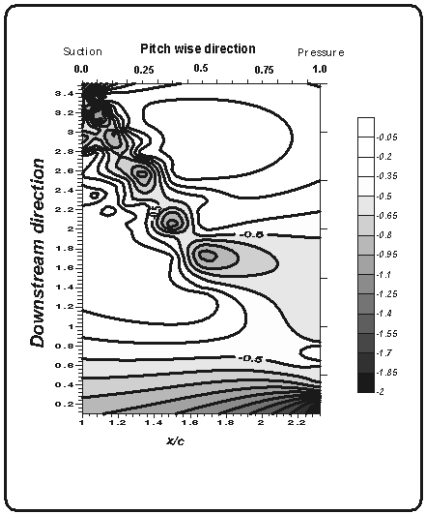

Fig. 7. Static Pressure Loss Coefficient Contours in Pitchwise Direction, BR (1.667).

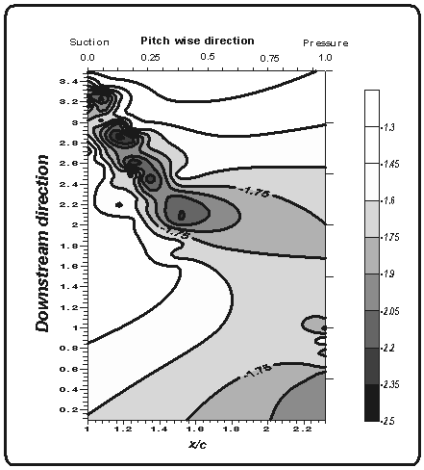

Fig. 8. Static Pressure Loss Coefficient Contours in Pitchwise Direction, BR (1.93).

The standard means of defining loss is the result of any flow feature that reduces the efficiency. Moreover, the majority of loss production thus occurs over

the suction surface, since the velocity is high, and the sudden rise in the loss coefficient at the transition point. The total pressure coefficient in the mixing region is presented in Figs. 9 to 11. These figures show C_{pt} contours in pitchwise direction. Three distinct core regions of high losses were observed. One core is close to the centre of the passage vortex, two cores at the suction side, one at the corner region and the other one at the midspan region.

Also these contours maps show the variation in C_{pt} quantities which are -1.2, -0.8 and 1.7 near the pressure side and 1.3, 1.95 and 3.45 at the vortex core near the suction side. The wake is elongated in downstream 1.18% for the chord and 0.7% of the pitchwise for the blowing ratio 1.58, 0.737% of the chord and 0.55% of the pitchwise for the blowing ratio 1.667 and 0.44% for the chord and 0.4% of the pitchwise for the blowing ratio 1.935.

The total pressure loss at the trailing edge increase with increase of the blowing ratios corresponds to the centre of the passage vortex. This result is as expected and agrees well with the results of [17]. The maximum loss regions occurred close to the suction surface. As the losses increase the flow travels downstream of the blade cascade due to mixing of the wake decayed the vortices and the growth of the end wall boundary layer. The domination of wake region for almost all the area downstream of blade trailing edge related to the persistence of momentum exchange between layers of higher rate of velocities (i.e., higher rate of momentum) with those having low rate of velocities due to the decay of flow near suction surface.

The core of passage vortex seems to migrate toward midspan at middle of the passage in the downstream direction. It is important to mention that the values of maximum C_{pt} always refer to the location of wake or vortex region that posse's high rate of losses. These remarkable results indicate that the total pressure loss coefficients are increased by 11%, 35% and 16% when compared with same results for the same cases done experimentally without using the trailing edge injection [blowing] obtained by [16].

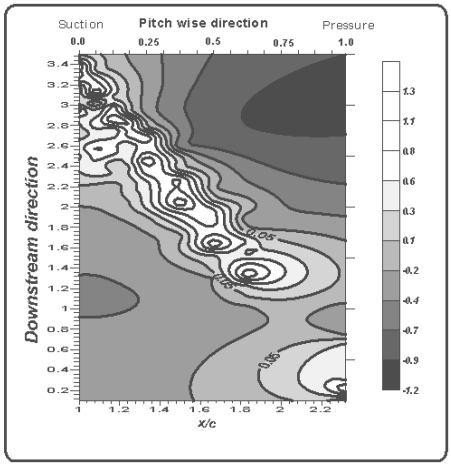

Fig. 9. Total Pressure Loss Coefficient Contours in Pitchwise Direction, BR (1.58).

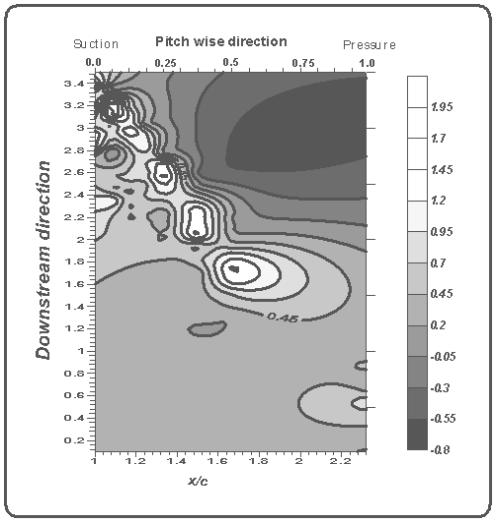

Fig. 10. Total Pressure Loss Coefficient Contours in Pitchwise Direction, BR (1.667).

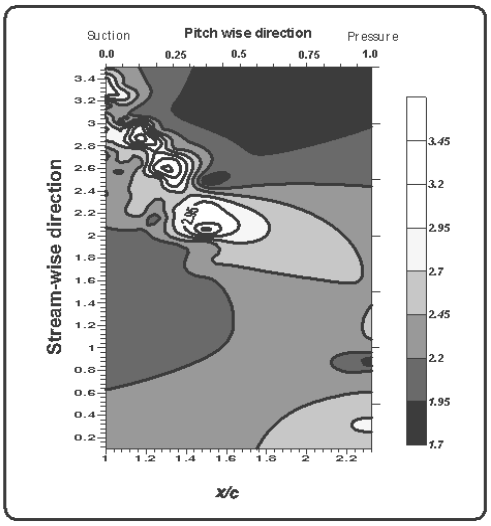

Fig. 11. Total Pressure Loss Coefficient Contours in Pitchwise Direction, BR (1.935).

4. Secondary Flow

Figures 12 to 14 show the contours maps of the secondary flow and velocity vectors, while Fig. 15 shows the primary flow, *u*, contours for three blowing ratio; 1.58, 1.667 and 1.935. These figures show the variation in secondary flow quantities of 19, 17, and 14 respectively.

It can be seen that the secondary flow decreases with increasing blowing ratio. Since the mass flow rate of the jets is high, the jets successfully push the vortex out of the passage without of impinging on the suction surface and this leads to successfully reducing secondary flow. It is important to notice that the appearance of any flow region having velocity, *w* other than zero will lead to the occurrence of secondary flow field. The same conclusion has drawn for the velocity component, *v*. The secondary flow components range near the suction side are between -12 and -16 m/s for blowing ratio 1.58 and -10 and -13 m/s and -8 and -11 m/s for blowing ratio 1.667 and 1.935 respectively. Recalling the subject of momentum transfer between layers having highest potential energy and zero kinetic energy, the exchange of momentum rate among former mentioned regions will continue to reveal the same trend of wake flow formation due to this rate of exchange. The results of the secondary flow contours of the present investigation agreed well with the results obtained by Charley [15].

Moving forward to the downstream the life distance exceeded the chord length. In this region there was a harmonization of secondary flow field in comparison to their values in the primary flow field (Fig. 15). This harmonization occurred at the stagnation flow (i.e., $u \sim 0$ m/s) showed a high limit of secondary flow component and this consolidates the vision of wake propagation downstream of blade cascade which possess more than one dimensional flow field component. These results agree well with results obtained by [17].

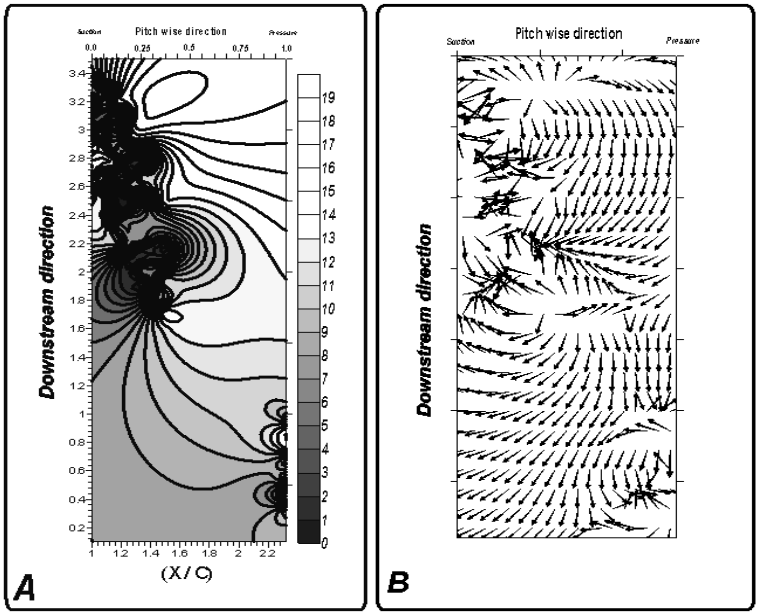

Fig. 12. Secondary Flow (A), and Velocity Vectors (B), (BR=1.58).

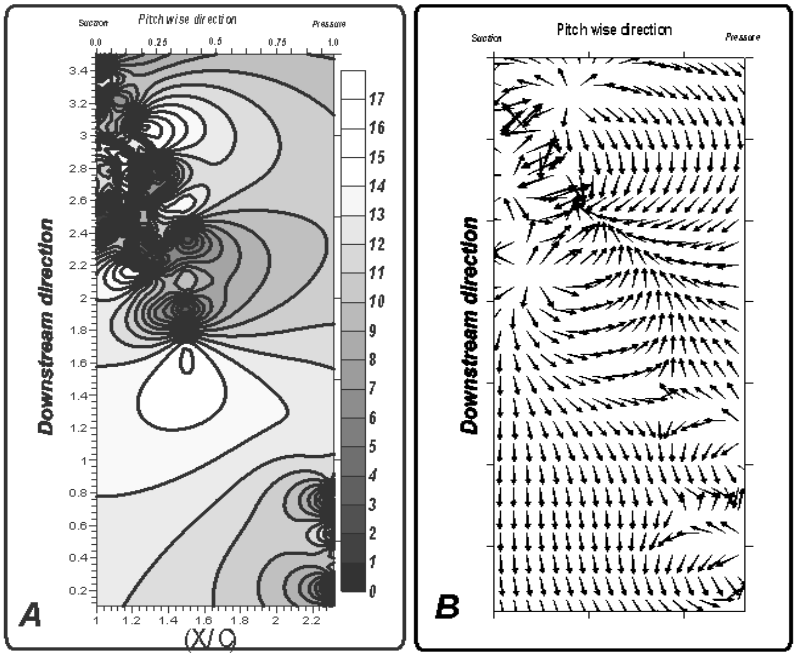

Fig. 13. Secondary Flow (A), and Velocity Vectors (B), (BR=1.667).

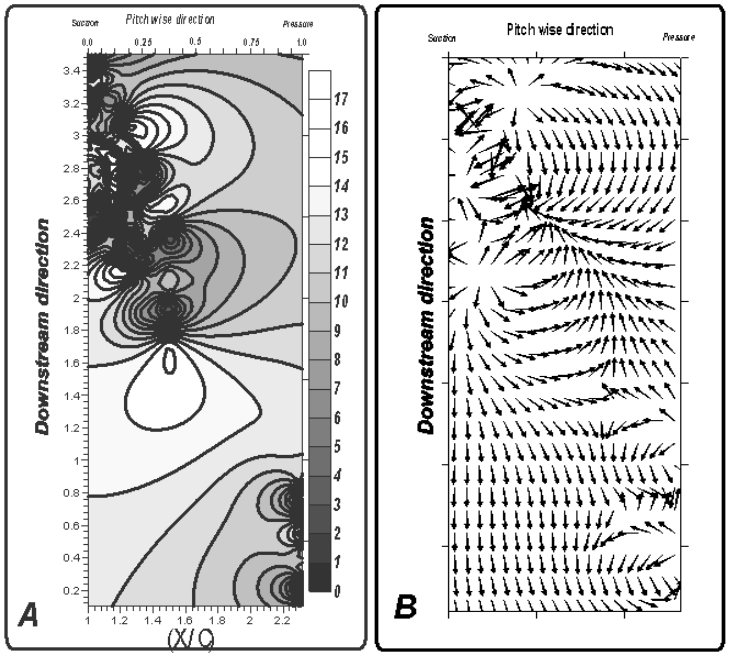

Fig. 14. Secondary Flow (A), and Velocity Vectors (B), (BR=1.935).

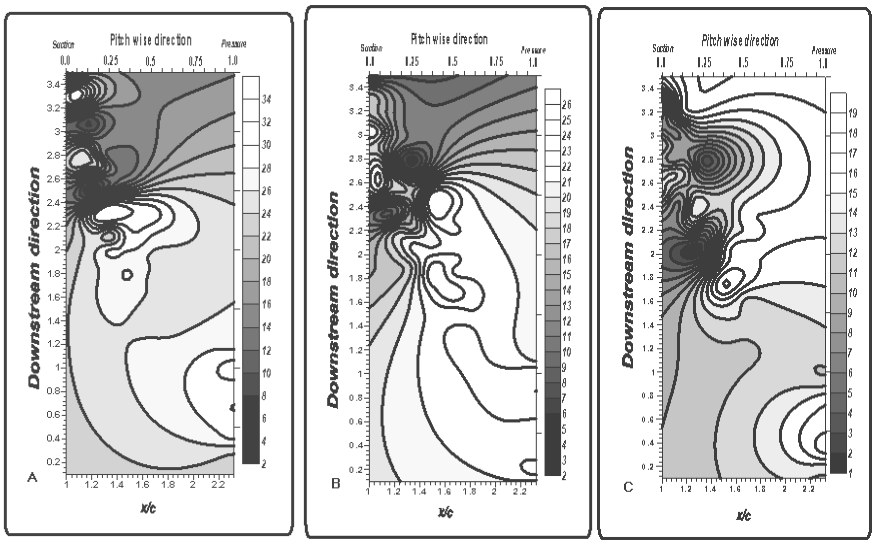

BR (1.58) **BR (1.667)** **BR (1.935)**

Fig. 15. Primary Flow, *U*, Contours.

5. Kinetic Energy Contours

The kinetic energy of primary and secondary flow is represented by equations shown below. These quantities considered per unit mass as:

$$\text{Total Flow Energy} = \frac{U^2}{2} \tag{5}$$

$$\text{Secondary Flow} = \sqrt{V^2 - x_{avg}^2} \tag{6}$$

Figures 16 to 18 show the turbulence kinetic energy with three blowing ratios. These figures show two regions of high-energy dissipation, one close to the suction side and this is quite obvious due to the generation of surface vortex and flow circulation, while the other region is located behind the blade trailing edge. These two regions life distances depend on the values of the blowing ratios and may be occurred due to the generation of the trailing edge vortex. In addition, any slight increase in vortex dissipation for accelerated flow associated with very strong random kinetic energy behaviour supports the previous conclusion about the generation of high mixing losses at high blowing ratio and therefore the wake life travels longer distance before the kinetic energies are dissipated. Also it can be noticed that the regions of maximum turbulent kinetic energies are located near the suction side of blade. In addition to that there is traces line in the downstream direction due to the effect of wake and vortices propagation. However, there is a lack of representation for the area lie below and above midpitch line, in which there is a disagreement with results obtained by [17] since at the present investigation there is no large quantities of turbulent kinetic energies appear between the traces of suction and the pressure sides.

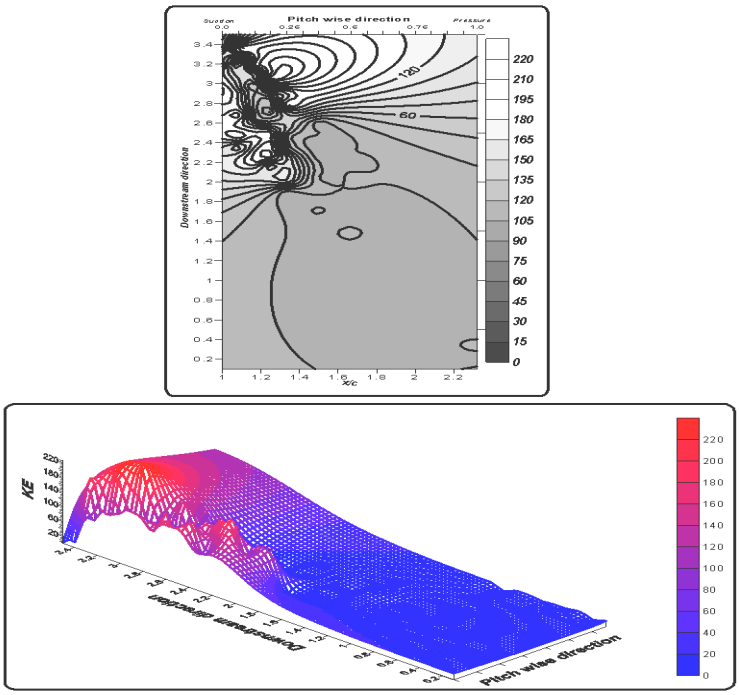

Fig. 16. Turbulence Kinetic Energy Contours and Kinetic Energy Distribution in Downstream and Pitchwise Directions, (BR=1.58).

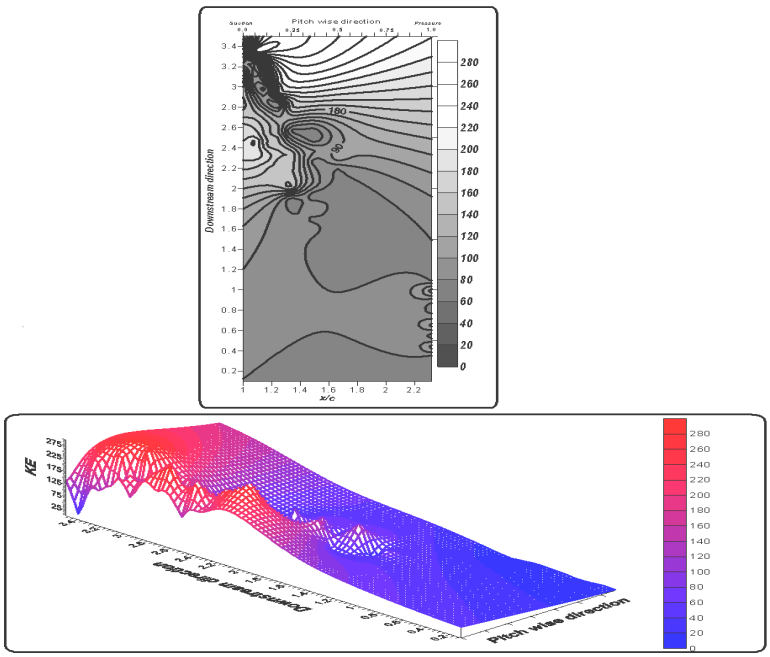

Fig. 17. Turbulence Kinetic Energy Contours and Kinetic Energy Distribution in Downstream and Pitchwise Directions, (BR=1.667).

In general, the existence of two adjacent regimes one with high and other with low turbulent kinetic energies will lead to the conclusion that these regimes exchange momentum because of wake convection as the flow progresses in downstream direction.

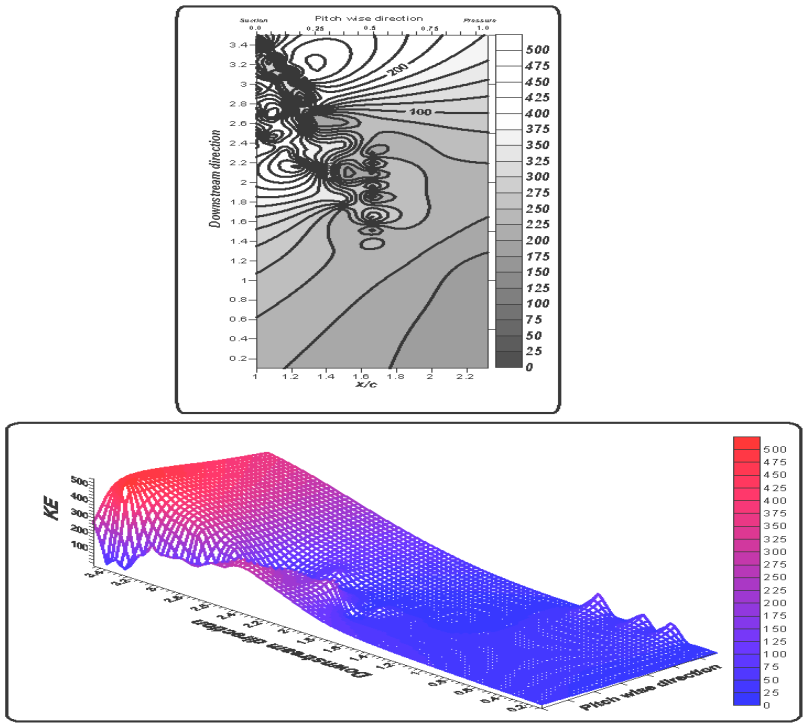

Fig. 18. Turbulence Kinetic Energy Contours and Kinetic Energy Distribution in Downstream and Pitchwise Directions, (BR=1.935).

6. Conclusions

An adequate solution to noise and vibration characteristics of turbomachinery cannot be found unless the mechanisms of the mixing losses process are to be cleared. From the work presented the wake mixing losses mechanisms of trailing edge cold jets issued into the hot cross flow may be understood according to the obtained experimental results.

- It is found that there is a certain harmonization between the secondary flow fields in comparison to their values in the primary flow field. This harmonization can be observed in the region of small primary flow or stagnation flow (i.e., u ~ 0 m/s).
- Flow structure in the wake is dominated by very strong random vortices close to the suction side and the trailing edge. The wake regions decrease in life distance with decreasing in blowing ratio.

- The core of the passage vortex may be dominated by any of the following three criteria, location of the maximum total pressure losses coefficient, location of the minimum static pressure losses coefficient and location of nominal centre of rotation of the secondary velocity vectors.
- The maximum total pressure loss coefficient reflects the concentration of wake region on three distinct regions of high losses.
- The pitchwise variation of static pressure coefficient contours was found to be much revealed in areas below midpitch. Therefore the rapid decay of the wake is conducted in the region lying below midpitch line due to the effect of inviscid core and trailing edge vortices. In addition, the static pressure coefficient contours are increased and have larger vortex core close to the suction surface, wherein the blowing ratio decreases.

Acknowledgement

We would like to express our deep appreciation to the head and staff of the Mechanical Engineering Department, University of Technology, Baghdad, Iraq and to all who contributed to the completion of this work, and also to our families for their patience and understanding.

References

1. Denton, J.D. (1993). Loss mechanisms in turbomachines. *ASME Journal of Turbomachinery*, 115(4), 621-656.
2. Wei, N. (2000). *Significance of loss models in aerothermodynamics simulation for axial turbines*. Ph.D. Thesis, Department of Energy Technology, Division of Heat and Power Technology, Royal Institute of Technology.
3. Arcangeli, L.; Surace, M.; Tarhi, L.; Coutandin, D.; and Zecchi, S. (2006). Correlative analysis of effusion cooling systems. *ASME Paper,* GT2006-90532.
4. Cerri, G .; Giovannelli, A.; Battisti, L.; and Fedrizzi, R. (2007). Advances in effusive cooling techniques of gas turbines. *Applied Thermal Engineering*, 27, 692- 698.
5. Hung, M.S.; Ding, P.P.; and Chen, P.H. (2009). Effects of injection angle orientation on concave and convex surfaces film cooling. *Experimental Thermal and Fluid Science*, 33(2), 292-305.
6. Langston, L.S.; Nice, M.L.; and Hooper, R.M. (1977). Three-dimensional flow within a turbine blade passage. *ASME Transactions, Journal for Engineering for Power*, 99(1), 21-28.
7. He, L. (1996). Unsteady flow in oscillating turbine cascade, part 1- linear cascade experiment. *ASME Paper*, 96-GT-374.
8. Friedrichs, S. (1997). *Endwall film-cooling in axial flow turbines*. Ph.D. Thesis, Engineering Department, Cambridge University.
9. Pope, A; and John, J.H. (1983). *Low speed wind tunnel*, John Wiley & Sons, New York, London.
10. Maskel, E.C. (1963). A theory of blockage effects on bluff bodies and stalled wings in a closed wind tunnel. *RAE Aero Report* 2685.

11. Sephered, I.C. (1981). A four-hole pressure probe for fluid flow measurement in three dimensions. *ASME Transactions, Journal of Fluids Eng*., 103(4), 590-594.
12. Schuiz, J.K. (2002). Measurement of magnitude and direction of hot gas flow in a fire compartment with a five-hole probe. *Fire Engineering*, University of Canterbury.
13. Kline, S.J.; and McClintock, F.A. (1953). Describing uncertainties in single sample experimental. *Mechanical Engineering Journal*, 75, 3-8.
14. Drost, U. (1994). *An experimental investigation of the corner stall behaviour of a linear compressor cascade at high angle of attack*. Diploma project, Swiss Federal, Institute of Technology, Lausanne.
15. Charley, F. (2002). *Measurement of hot gas flow in a fire compartment*. M.Sc. Thesis, University of Canterbury.
16. Ali, S.A.S. (2007). *Investigation of flow through axial turbine blade passage*. Ph.D. Thesis, Al-Nahrain University, Baghdad, Iraq.
17. Moore J.; and Adhye, R.Y. (1985). Secondary flows and losses downstream of a turbine cascade. *ASME Journal of Engineering for Gas Turbine and Power*, 107, 961-968.